

Supporting information

A cost-effective, stable, magnetically recyclable photocatalyst of ultra-high organic pollutant degradation efficiency: SnFe_2O_4 nanocrystals from a carrier solvent assisted interfacial reaction process

*Kuan-Ting Lee and Shih-Yuan Lu**

Department of Chemical Engineering, National Tsing Hua University, Hsinchu 30013,

Taiwan

*Email : SYLu@mx.nthu.edu.tw

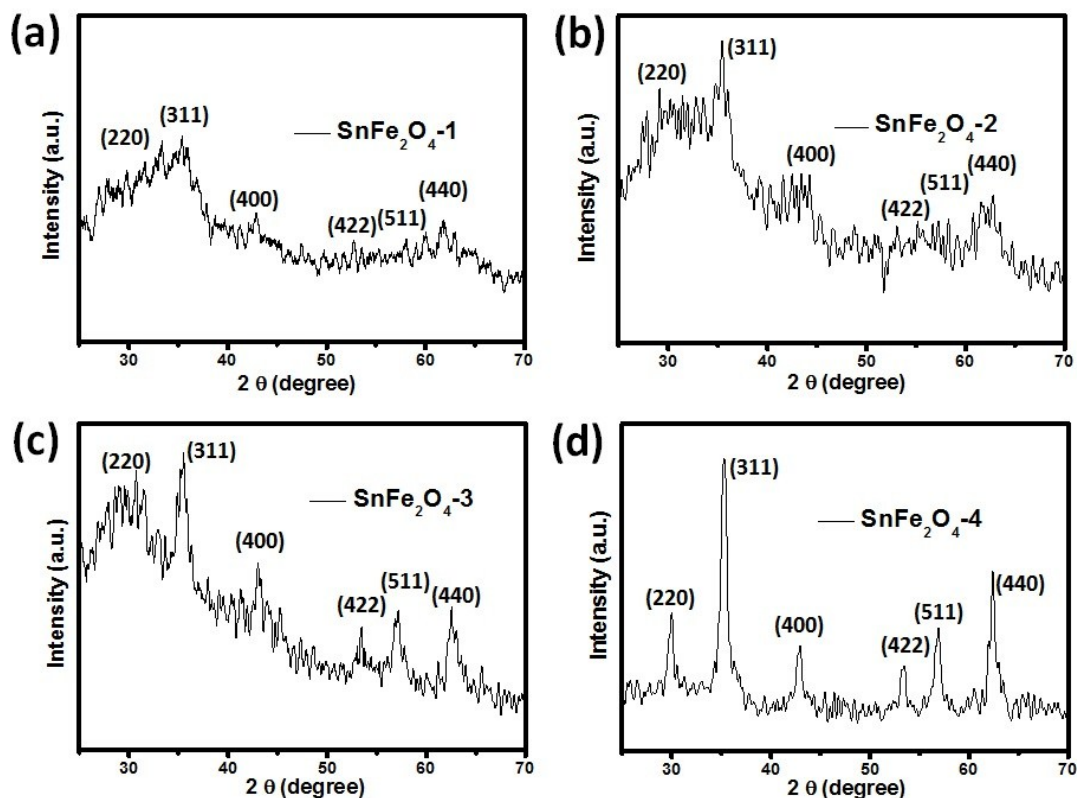


Fig. S1. XRD patterns of samples SnFe_2O_4 -1 to SnFe_2O_4 -4.

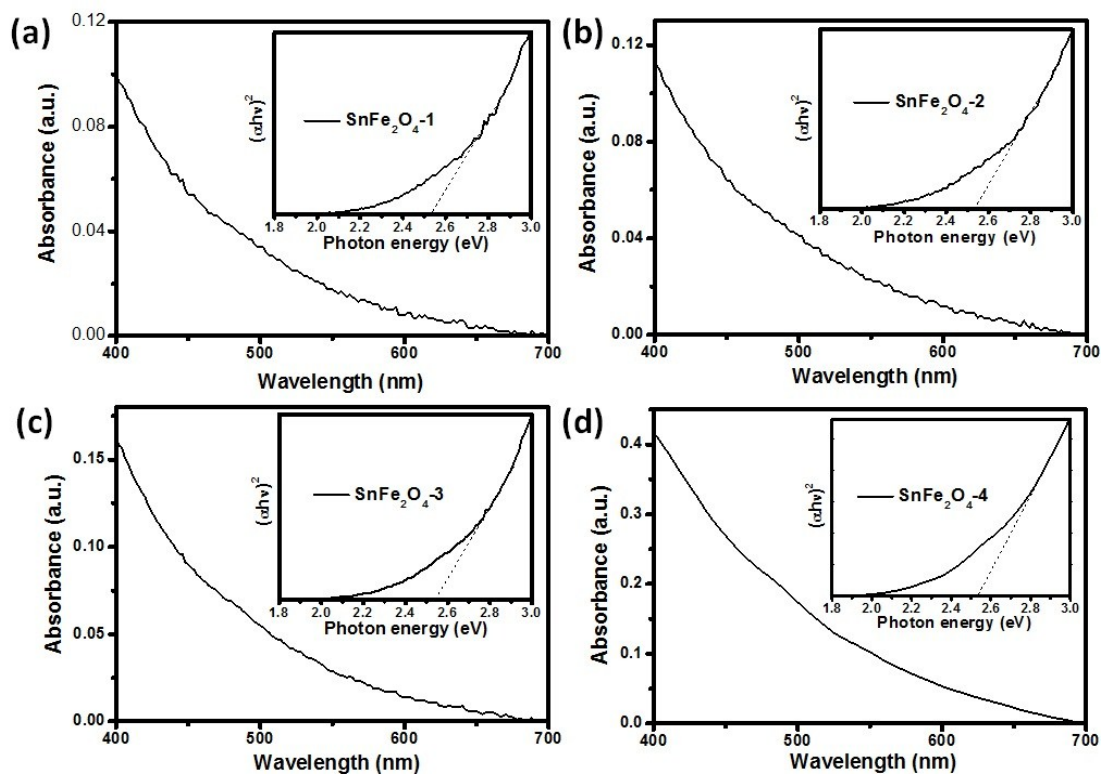


Fig. S2. UV-visible spectrum of samples SnFe₂O₄-1 to SnFe₂O₄-4. Inset shows $(\alpha h\nu)^2$ vs. photon energy plot for bandgap determination.

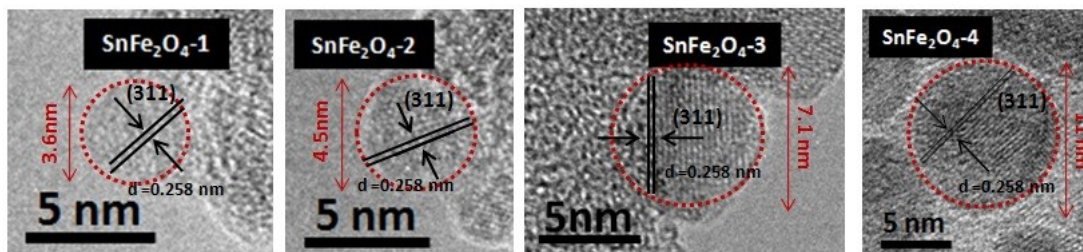


Fig. S3. HRTEM images of samples SnFe₂O₄-1 to SnFe₂O₄-4.

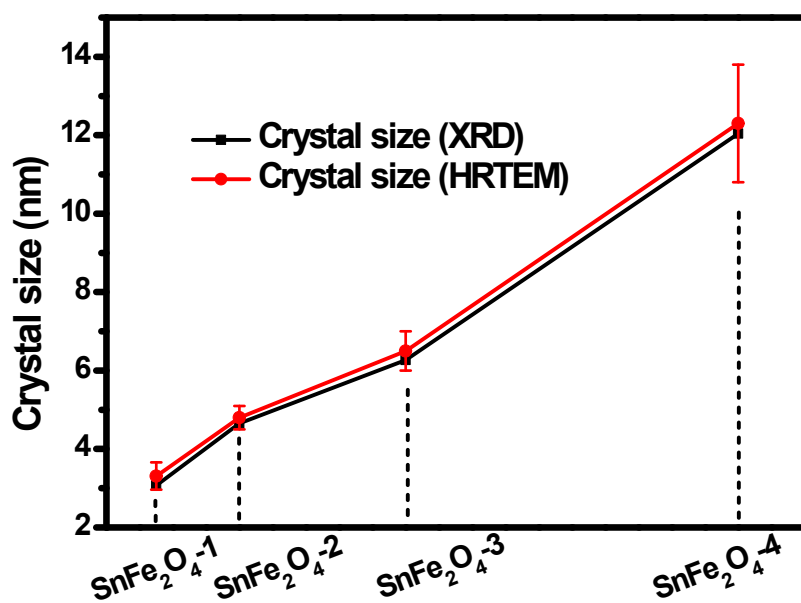


Fig. S4. Comparison of nanocrystal sizes for all four SnFe₂O₄ samples, as determined from XRD patterns and HRTEM images.

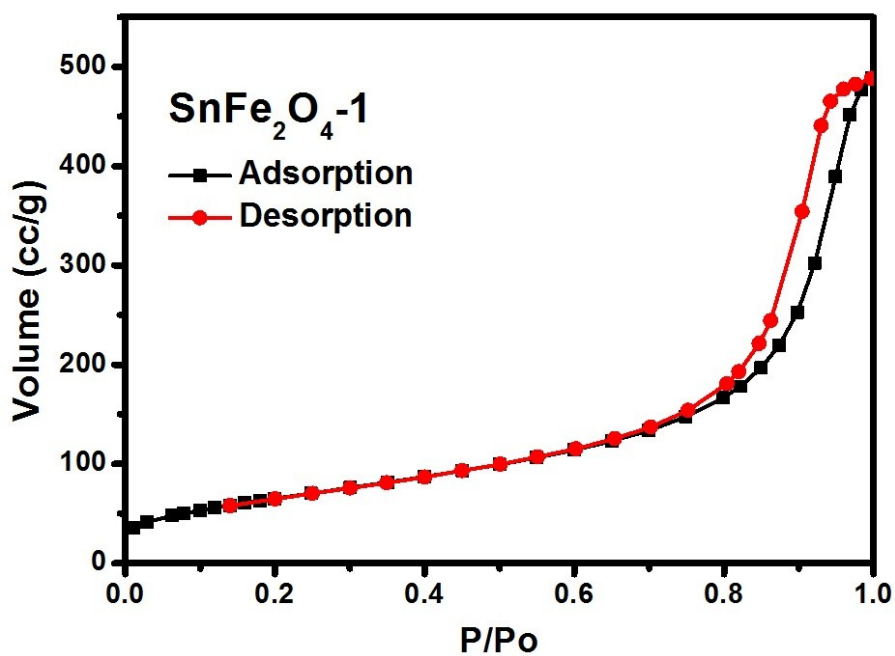


Fig. S5. N₂ adsorption/desorption isotherms of sample SnFe₂O₄-1.

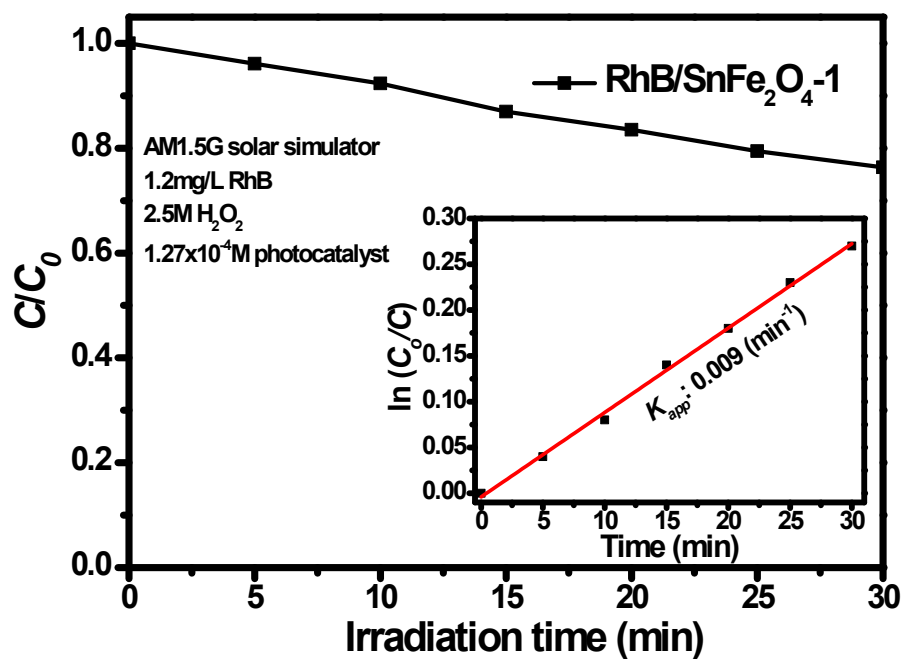


Fig. S6. C/C_0 versus time curve for RhB solution containing sample SnFe₂O₄-1 without H₂O₂ addition. Inset shows determination of K_{app} .

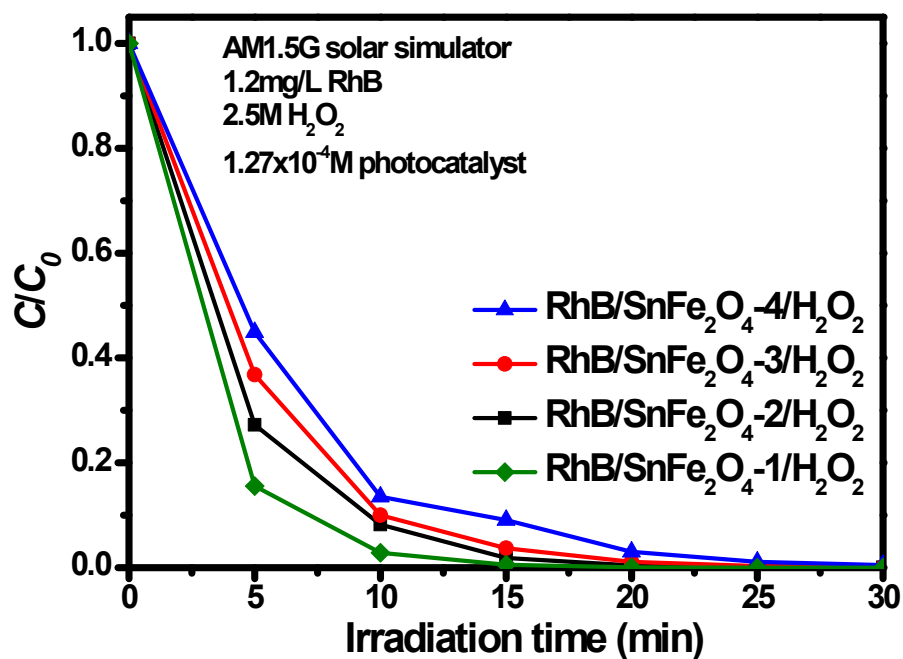


Fig. S7. C/C_0 versus time curves for RhB solution containing samples SnFe₂O₄-1 to SnFe₂O₄-4 with H₂O₂ addition.

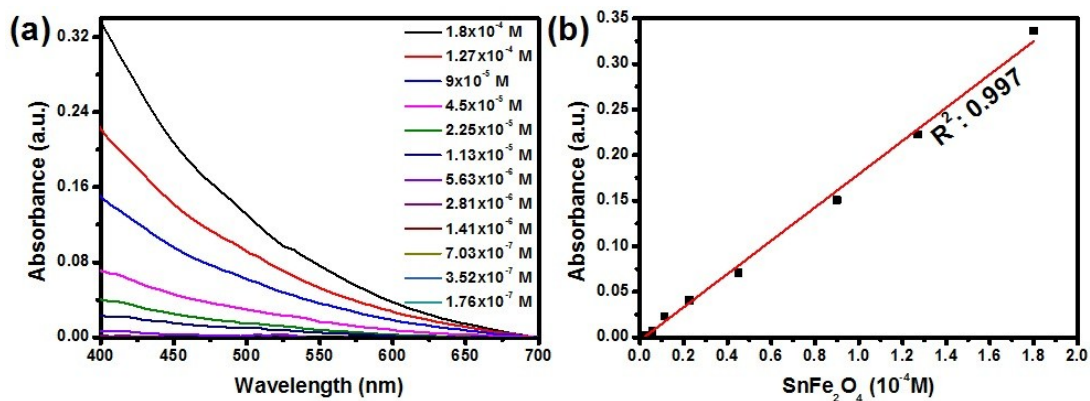


Fig. S8. (a) Absorption spectra of sample SnFe₂O₄-1 suspensions at selected concentrations, (b) correlation curve of absorbance of SnFe₂O₄ suspension at 400 nm vs. SnFe₂O₄ concentration.

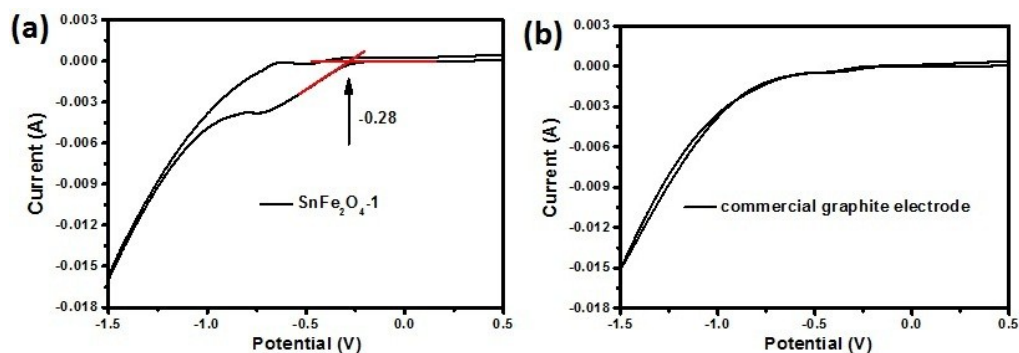


Fig. S9. Cycling voltammograms recorded for (a) sample SnFe₂O₄-1, (b) commercial graphite electrode.

Table S1 Atomic ratios of Fe vs. Sn of samples SnFe₂O₄-1 to SnFe₂O₄-4.

| Photocatalyst | Fe / Sn (atomic ratio) |
|-------------------------------------|------------------------|
| SnFe ₂ O ₄ -1 | 2.08 |
| SnFe ₂ O ₄ -2 | 2.19 |
| SnFe ₂ O ₄ -3 | 2.03 |
| SnFe ₂ O ₄ -4 | 2.34 |

Table S2 Grain sizes and coercivities of samples SnFe₂O₄-1 to SnFe₂O₄-4.

| Photocatalyst | Grain size (nm) | Coercivity (Oe) |
|-------------------------------------|-----------------|-----------------|
| SnFe ₂ O ₄ -1 | 3.1 | 7.5 |
| SnFe ₂ O ₄ -2 | 4.7 | 10 |
| SnFe ₂ O ₄ -3 | 6.3 | 22 |
| SnFe ₂ O ₄ -4 | 12.0 | 4.0 |

Table S3 Compilation of apparent reaction rate constants for RhB degradation in Fenton-like processes.

| Reference | Type of catalyst | Source of light | Concentration of RhB (mg/L) | Concentration of catalyst(M) | Apparent reaction rate constant; K_{app} (min ⁻¹) |
|------------------|----------------------------------|--|-----------------------------|------------------------------|---|
| [S1] | BiVO ₄ | 350W Xe lamp, simulated sunlight | 9.58 | 3.09×10 ⁻³ | 0.098 |
| This work | SnFe ₂ O ₄ | 150W Xe lamp, simulated sunlight | 10 | 1.27×10 ⁻⁴ | 0.13 |
| [S2] | BiFeO ₃ | 500 W Halogen lamp with a cutoff filter (> 420 nm) | 4.79 | 1.6×10 ⁻³ | 0.056 |
| [S3] | g-C ₃ N ₄ | 500 W Halogen lamp with a cutoff filter (> 420 nm) | 4.79 | 0.5 (g/L) | 0.044 |

| | | | | | |
|------------------|--|---|------|-----------------------|------------|
| [S4] | EuFeO ₃ | 500 W Xe lamp with a cutoff filter (> 420 nm) | 5 | 3.9×10 ⁻³ | 0.002 |
| [S5] | Bi ₂ WO ₆ /Cu ⁰ | 500 W Xe lamp with a cutoff filter (> 420 nm) | 4.79 | 1.4×10 ⁻³ | 0.03 |
| This work | SnFe ₂ O ₄ | 150W Xe lamp, simulated sunlight /with a cutoff filter (> 422 nm) | 5 | 1.27×10 ⁻⁴ | 0.21/ 0.15 |

Table S4. Band structure parameters of SnFe₂O₄ NCs.

| sample | E_{red} (V) | LUMO ^a (eV) | HOMO ^b (eV) | λ_{abs} ^c (nm) | E_{g} ^d (eV) |
|-------------------------------------|----------------------|------------------------|------------------------|--|----------------------------------|
| SnFe ₂ O ₄ -1 | -0.28 | -4.43 | -6.96 | 505 | 2.53 |

^aDetermined by Eq. (1). ^bDetermined from LUMO and band gap energy. ^cMeasured by UV–visible absorption spectrum. ^dEstimated from UV–visible absorption spectrum.

Experimental determination of conduction band position of SnFe₂O₄ NCs:

Here, we determine the conduction band position of SnFe₂O₄ NCs with cyclic voltammetry analyses. The working electrode was prepared by drop-casting ethanolic suspension of SnFe₂O₄ NCs onto a graphite electrode followed by drying at 60 °C. The counter electrode was Pt coil, and Ag/AgCl served as the reference electrode. The cyclic voltammograms were recorded in an electrolyte of 0.1 M Na₂SO₄(aq) with a negative scan starting from 0.5 to -1.5 V and then back to 0.5 V at a scan rate of 30 mV/s. The LUMO energy (E_{LUMO}) of electroactive materials can be estimated from the onset reduction potential (E_{red}), according to the following equation^[S6,S7]

$$E_{\text{LUMO}} = -(E_{\text{red}} + 4.71) \text{ eV} \quad (1)$$

Here, the onset potential is referenced to the Ag/AgCl electrode. The value of 4.71 represents the difference between the vacuum level potential of the normal hydrogen electrode (NHE) and the potential of the Ag/AgCl electrode versus NHE.^[S8,S9] We started from 0.5 V and proceeded with a negative potential scan from 0.5 to -1.5 V and then back to 0.5 V. The onset reduction potentials of sample SnFe₂O₄-1 was thus determined to be -0.28 V as shown in Fig. S9(a). A commercial graphite electrode

was taken as a control, and no reduction peak can be identified under the same testing condition, as shown in Fig. S9(b). The results of relevant band structure data were summarized in Table S4.

References:

- [S1]. M. Ge, L. Liu, W. Chen, Z. Zhou, *CrystEngComm*, 2012, **14**, 1038-1044.
- [S2]. J. An, L. Zhu, Y. Zhang, H. Tang, *Journal of Environmental Sciences*, 2013, **25**, 1213-1225.
- [S3]. Y. Cui, Z. Ding, P. Liu, M. Antonietti, X. Fu, X. Wang, *Phys. Chem. Chem. Phys.*, 2012, **14**, 1455-1462.
- [S4]. L. Ju, Z. Chen, L. Fang, W. Dong, F. Zheng, M. Shen, *J. Am. Ceram. Soc.*, 2011, **94**, 3418-3424.
- [S5]. J. Xu, W. Wang, E. Gao, J. Ren, L. Wang, *Catalysis Communications*, 2011, **12**, 834-838.
- [S6] K. G. Deepa, J. Nagaraju, *Mater. Sci. Eng. B*, 2012, **177**, 1023-1028.
- [S7] K. T. Lee,, S. Y. Lu, *J. Phys. Chem. C*, 2014, **118**, 14457-14463.
- [S8] C. Karunakaran, J. Jayabharathi, K. Jayamoorthy, K. B. Devi, *Sens. Actuators B*, 2012, **168**, 263-270.
- [S9] S. H. Chang, M. Y. Chiang, C. C. Chiang, F. W. Yuan, C. Y. Chen, B. C. Chiu, T. L. Kao, C. H. Lai, H. Y. Tuan, *Energy Environ. Sci.* 2011, **4**, 4929-4932.